Scientific paper

# Synthesis, Structure, Thermal Decomposition and Computational Calculation of Heterodinuclear Ni<sup>II</sup> – Zn<sup>II</sup> Complexes

Yaprak Gürsoy Tuncer,¹ Hasan Nazır,¹ Kübra Gürpınar,¹ Ingrid Svoboda,² Nurdane Yılmaz,³ Orhan Atakol¹ and Emine Kübra İnal¹,\*

<sup>1</sup> Ankara University, Faculty of Science, Department of Chemistry, 06100, Ankara, Turkey

<sup>2</sup> TU-Darmstadt, Materialwissenschaft, Strukturforschung, Alarich-Weiss Strasse 2, 64287, Darmstadt, Germany

<sup>3</sup> Kastamonu University, Faculty of Education, Department of Mathematics and Science Education, 37200, Kastamonu, Turkey

\* Corresponding author: E-mail: inal@science.ankara.edu.tr

Received: 09-07-2021

#### **Abstract**

Mononuclear NiL complex was prepared by the use of bis-N,N'-salicylidene-1,3-propanediamine and Ni(II) salts. NiL was treated with  $ZnBr_2$  and pyrazole and 3,5-lutidine coligands in a dioxane medium to prepare the following diheter-onuclear complexes:  $[NiL \cdot ZnBr_2 \cdot (pyrazole)_2]$  and  $[NiL \cdot ZnBr_2 \cdot (3,5-lutidine)_2]$ . The complexes were characterized by elemental analysis, TG, IR and mass spectrometry. The effects of heterocyclic one- and two- nitrogen atoms containing co-ligands were also examined. Theoretical formation enthalpies, dipole moments and the relative levels of HOMO and LUMO energies were determined by the use of Gaussian09 program. The occupancy levels of the atomic orbitals were determined by the NBO analysis of Gaussian09. The effect of pyrazole and lutidine upon the complex formation was evaluated by the use of X-ray diffraction, TG and theoretical calculations. NiL complex with lutidine forms a square pyramidal conformation since lutidine is a much stronger coligand than pyrazole.

 $\textbf{Keywords:} \ Salpn\ type\ ligand;\ Ni(II)-Zn(II)\ dinuclear\ complex;\ square-pyramidal\ coordination;\ thermal\ decomposition;\ heterocyclic\ coligand$ 

#### 1. Introduction

Bis-N,N'-salicylidene-1,3-propanediamine (LH<sub>2</sub>) has been known to give homo- and heteropolynuclear complexes with Fe(II), Co(II), Ni(II), Cu(II), Zn(II) and Cd(II) ions since 1990.<sup>1-3</sup> This compound that is classified as a Schiff base and a tetradentate ONNO type ligand gives heterodinuclear complexes with Lewis acids such as  $ZnCl_2$  and  $ZnBr_2$ , and polynuclear complexes with a  $\mu$ -bridge forming co-ligands such as acetate,<sup>4-9</sup> formate,<sup>10,11</sup> nitrate,<sup>7,12,13</sup> nitrite,<sup>14</sup> benzoate,<sup>15,16</sup> pseudohalogen or azides.<sup>17-20</sup> In complexes prepared with Lewis acids, it is very common that one or two solvent molecules enter the coordination sphere. The complex maintains its existence with the coordination of solvent molecules. If these solvent molecules are thermally removed from the structure, the dinuclear structure decomposes.<sup>21-23</sup>

In addition to LH<sub>2</sub> ligand giving mononuclear NiL and CuL complexes with Ni(II) and Cu(II), the resulting mononuclear complexes may be utilized to obtain polynuclear complexes. The molecular models of NiL and CuL mononuclear complexes were first reported in 1985.  $^{24}$  In this study, it was determined that Cu(II) complex had a squashed tetrahedral and Ni(II) complex a square planar coordination sphere. If there are Lewis acids present in the medium, these Lewis acids are coordinated especially to NiL mononuclear complex through phenolic oxygens. As a result, Lewis acids withdraw electrons from NiL unit which decreases electron density upon Ni(II) and enables it to coordinate the solvent molecules or coligands present in the medium (Figure 1).

Mononuclear NiL complex can form a square pyramidal coordination sphere by coordinating  $\rm H_2O$  molecule

Figure 1. Dinuclear complex formation with the effect of Lewis acid in the medium.

if there is no Lewis acid in the medium. <sup>25</sup> Generally, trinuclear complexes are formed if there are coligands capable of establishing  $\mu$ -bridges (Y) such as HCOO<sup>-</sup>,  $C_6H_5COO^-$ ,  $AcO^-$ ,  $NO_2^-$ ,  $NO_3^-$ . <sup>4–16</sup> In these trinuclear complexes, NiY<sub>2</sub> is located in the center. Terminal groups are the solvent molecules such as DMF or dioxane coordinated by NiL. <sup>4–9,26</sup> If coligands containing more than one nitrogen donor, such as pyrazole or dicyandiamide, are added to the medium, polynuclear complexes are formed. <sup>27</sup>

This study is devoted to determine the type of coordination sphere formed by NiL and ZnBr2 together with one or two nitrogen-containing coligands. In a previous study, it was reported that NiL mononuclear complex forms a square pyramidal or octahedral coordination sphere with ZnCl<sub>2</sub>, ZnBr<sub>2</sub>, and 4-methylpyridine (4-picoline).28 Based upon the picoline concentration there formed a square pyramidal complex with a [NiL·ZnCl<sub>2</sub>· (4-picoline)] or an octahedral coordination sphere with [NiL·ZnBr<sub>2</sub>·(4-picoline)<sub>2</sub>] stoichiometries. The major target of this study is to investigate the complexes formed if the reaction medium contains more than one heteroatom such as pyrazole and triazole. In this context, the coligands chosen were multi heteroatom containing pyrazole and a single heteroatom containing 3,5-lutidine, complexes were prepared in DMF and dioxane media.

The complexes obtained were characterized by IR spectroscopy, elemental analysis, mass spectrometry and thermogravimetric analysis. The goal of the study was to prepare two complexes and elucidate the differences between their thermal behavior. Two complexes designed for the study were obtained as single crystals, their molecular models and unit cell structures were determined by X-ray diffraction methods. The determination of the number of pyrazoles coordinated by NiL unit and their locations was one of the major targets of the study since pyrazole coordination has various isomerization possibilities. The main purpose of the study is to investigate the difference between pyrazole complexes containing multiple nitrogen donors and lutidine complexes containing a single nitrogen donor. In previous studies, it has been reported that NiL and pyrazole give a polynuclear complex. As a result, both ligands give mononuclear complexes, the interesting thing is that the difference between them is obtained by thermogravimetric analysis, not by XRD study. The removal temperatures of the coligands from the structure enabled us to evaluate the strengths of the ligands upon the molecular structure.

The variation in the thermal behavior of complexes  $[NiL \cdot ZnBr_2 \cdot (pyrazole)_2]$  (1) and  $[NiL \cdot ZnBr_2 \cdot (3,5-lutidine)_2]$  (2) was elucidated by thermal analysis and theoret-

ical calculations were carried out upon the molecular structures, by using Gaussian 09 software. With natural bond analysis (NBO) in Gaussian 09 program, the occupancy levels of d orbitals of the central atoms, the molecular dipole moment of the complexes, the electron distributions, the relative energy levels of the highest occupied molecular orbital (HOMO) and the lowest unoccupied molecular orbital (LUMO), the energy difference between HOMO and LUMO were calculated. The values of the theoretical and experimental bond lengths and bond angles were compared. All the theoretical results were interpreted according to the strength of the ligands.

#### 2. Experimental

All the reagents used in the study were supplied from Sigma-Aldrich and used without further purification. In this study, Shimadzu IRAffinity-1 FTIR spectrometer equipped with three reflectional ATR units was used for IR spectra with 4 cm<sup>-1</sup> accuracy. C, H, and N analyses were performed on Eurovector 3018 CHNS analyzer. Metal analyses were carried out on GBC Avanta PM Model atomic absorption spectrometer using FAAS mode. Complex (2-3 mg) was dissolved in 1 mL HNO<sub>3</sub> (63%) with heating, diluted to 100 mL and given to nebulizer of atomic absorption spectrometer for metal analysis. The mass spectra of the ligands were obtained by Shimadzu QP2010 Plus GCMS apparatus equipped with a direct inlet (DI) unit with an electron impact ionizer (EI). DI temperature was varied between 40-300 °C and ionization was carried out with electrons with 70 eV energy. The NMR spectra were recorded on the Bruker Ultrashield 300 MHz NMR spectrometer using  $d_6$ -DMSO solution as a solvent. The thermogravimetric analyses were carried out by Shimadzu DTG 60H. In thermogravimetric analyses, the temperature was varied between 30-600°C. These analyses were performed at 5, 10, 15, 20 and 25 °C min<sup>-1</sup> heating rates and under N2 atmosphere in Pt pans. The calibration of the instrument was done with metallic In and Zn.

## 2. 1. Preparation of bis-N,N'-salicylidene-1,3-propanediamine (LH<sub>2</sub>)

The Schiff base was prepared *via* condensation reaction in EtOH using 2-hydroxybenzaldehyde and 1,3-diaminopropane. 2-hydroxybenzaldehyde (0.1 mol, 12.20 g) was dissolved in 120.0 mL of warm EtOH, then 0.05 mol (3.70 g) of 1,3-diaminopropane was added to and heated up to the boiling point. The mixture was left aside for 4–5 h and yellow crystals were precipitated, then the crystals were filtered and dried in air (25.90 g), yield: 91%, mp: 58 °C (determined by TG). Anal. Calcd for  $C_{17}H_{18}N_2O_2$ : C, 72.32; H, 6.43; N, 9.92. Found: C, 71.95; H, 6.33; N, 10.09. IR v, cm<sup>-1</sup>: 2627 (OH), 3021–3019 (CH), 2929-2862 (CH), 1629 (C=N), 1608 (C=C), 1274-1151 (C–O),

762 (CH).  $\lambda_{max}$ : 243nm,  $\epsilon$ : 7045 dm³ mol⁻¹ cm⁻¹ in DMSO,  $\lambda_{max}$ : 242 nm,  $\epsilon$ : 7865 dm³ mol⁻¹ cm⁻¹ in MeOH. ¹H NMR (CH₃COCH₃-d₆)  $\delta$  13.51 (s, 1H) (O−H), 8.60 (s, 1H) (−CH=), 7.43 (d, J = 1.8 Hz) (H<sub>Ar</sub>), 7.32 (t, J = 1.8 Hz) (H<sub>Ar</sub>), 6.88 (t, 1.8 Hz) (H<sub>Ar</sub>), 3.68 (t, J = 7.2 Hz) (N−CH₂−), 2.01 (p, J = 7.2 Hz) (−CH₂−). ¹³C NMR (CH₃COCH₃-d₆)  $\delta$  166.6, 161.1, 132.7, 132.1, 119.1, 118.9 (C<sub>Ar</sub>), 116.9 (−C=N), 58.5 (N−CH₂−), 31.9 (−CH₂−). MS m/z: 282 [M]⁺, 161 [HO−C₆H₄−CH=N−CH₂−CH₂]⁺, 148 [HO−C₆H₄−CH=N−CH₂]⁺, 120 [HO−C₆H₄−CH=N]⁺, 107 [HO−C₆H₄−CH=N−CH₂]⁺, 77 [C₆H₅]⁺.

#### 2. 2. Preparation of the Complexes

The complexes were prepared in two steps. The mononuclear NiL complex synthesized in the first step was converted into the dinuclear complex in DMF or dioxane medium in the second step.

### 2. 2. 1. Preparation of Mononuclear Complex (NiL)

NiL was prepared by ammonia in an ethanol solution of LH<sub>2</sub> and NiCl<sub>2</sub> · 6H<sub>2</sub>O outlined in the literature.<sup>33</sup> 0.01 mol of LH<sub>2</sub> (2.82 g) was dissolved in 100.0 mL of hot EtOH under stirring. 10.0 mL of concentrated ammonia (20%) solution was added and the mixture was heated up to boiling temperature. A solution of 0.01 mol NiCl<sub>2</sub>. 6H<sub>2</sub>O (2.36 g) in 30.0 mL hot water was added to this mixture. After the mixture was left on the bench for an hour, the light green precipitate of NiL·NH3 was filtered and dried at 150 °C for 4-5 h (3.45 g), yield: 95%, mp: 311 °C. The light green crystals are coordinatively ammonia bonded and leaves ammonia at 150 °C, the color of the complex changes to brown (NiL). The brown complex was recrystallized in EtOH:dioxane mixture (1:1, v/v). Anal. Calcd for  $C_{17}H_{16}N_2O_2Ni$ : C, 60.28; H, 4.76; N, 8.27; Ni, 17.33. Found: C, 60.55; H, 3.17; N, 7.93; Ni, 17.19. IR v, cm<sup>-1</sup>: 3061-3030 (CH), 2922-2866 (CH), 1607 (C=N), 1589-1541 (C=C), 1475 (CH), 1228-1124 (C-O), 725-744 (CH). MS m/z: 340 (isotope peak, because of  $^{60}$ Ni isotope), 338 [M]<sup>+</sup> (base peak), 219 [Ni-O-C<sub>6</sub>H<sub>4</sub>-CH=NH-CH<sub>2</sub>- $CH_2-CH_2$ <sup>+</sup>, 205 [Ni-O-C<sub>6</sub>H<sub>4</sub>-CH=NH-CH<sub>2</sub>-CH<sub>2</sub>]<sup>+</sup>, 179  $[Ni-O-C_6H_4-CH=NH]^+$ , 134  $[O-C_6H_4-CH=NH CH_2$ ]<sup>+</sup>, 107 [HO-C<sub>6</sub>H<sub>4</sub>-CH<sub>2</sub>]<sup>+</sup>, 58 [Ni]<sup>+</sup>.

## 2. 2. 2. Preparation of Complex 1, [NiL · ZnBr<sub>2</sub> · (pyrazole)<sub>2</sub>]

0.001~mol of NiL (0.340 g) was dissolved in 50.0 mL hot DMF under stirring and heated up to  $100{-}110~^{\circ}\mathrm{C}.$  A solution of 0.001 mol  $ZnBr_2$  (0.226 g) and 0.002 mol pyrazole (0.140 g) in 30.0 mL hot MeOH was added to this solution. The mixture was left on the bench for 2–4 days at room temperature. The light purple crystals were filtered

and dried in air (0.41 g), yield: 58%. mp: 190 °C (decomposition). Anal. Calcd for  $C_{23}H_{24}Br_2N_6NiO_2Zn$ : C, 39.56; H, 3.18; N, 12.03; Ni, 8.40; Zn, 9.36; Br, 22.88. Found: C, 40.17; H, 3.27; N, 11.93; Ni, 8.01; Zn, 9.47; Br; 21.83. IR  $\nu$ , cm<sup>-1</sup>: 3335 (NH), 3120 (CH), 3034–3017 (CH), 2929–2861 (CH), 1631–1618 (C=N), 1593-1552 (C=C), 1475 (CH), 1298–1118 (C–O), 759 (CH). MS m/z: 338 (molecular peak of NiL and base peak), 179, 132, 107, 77, 58, 44.

## 2. 2. 3. Preparation of Complex 2, [NiL · ZnBr<sub>2</sub> · (3,5-lutidine)<sub>2</sub>]

This complex was prepared as given above using 0.001 mol of NiL (0.340 g), 0.001 mol of  $ZnBr_2$  (0.226 g) and 0.002 mol of 3,5-lutidine (0.220 g). The mixture was left on the bench for 2–4 days at room temperature. The light purple crystals were filtered and dried in air (0.59 g), yield: 76%. mp: 157 °C (decomposition). Anal. Calcd for  $C_{31}H_{34}Br_2N_4NiO_2Zn$ : C, 44.52; H, 4.42; N, 7.68; Ni, 8.06; Zn, 8.97; Br, 21.93. Found: C, 40.08; H, 3.93; N, 7.35; Ni, 7.73; Zn, 8.59; Br, 21.81. IR v, cm<sup>-1</sup>: 3031–3009 (CH), 2921–2865 (CH), 1618 (C=N), 1595-1550 (C=C), 1475 (CH), 1301–1107 (C–O), 752 (CH). MS m/z: 338 (molecular peak of NiL), 107 (coligand and base peak), 92, 79, 71, 58, 43.

#### 2. 3. X-Ray Crystallography

A single crystals of  $[NiL \cdot ZnBr_2 \cdot (pyrazole)_2]$  (1) and  $[NiL \cdot ZnBr_2 \cdot (3,5-lutidine)_2]$  (2) were analyzed on Oxford Diffraction Xcalibur Single Crystal X-ray Diffractometer with a sapphire CCD detector using MoK $\alpha$  radiation ( $\lambda$  = 0.71073 Å) operating in  $\omega/2\theta$  scan mode. The unit-cell dimensions were determined and refined by using the angular settings of 25 automatically centered reflections in  $2.588^{\circ} \le \theta \le 26.369^{\circ}$  for 1 and  $2.556^{\circ}-27.894^{\circ}$  for 2. The data was collected at 293(2) K. The empirical absorption corrections were applied by the semi-empirical method via the CrysAlis CCD software.30 The model was obtained from the results of the cell refinement and the data reductions were carried out using the solution software SHELXL 2014-6.31 The structure of the complexes was solved by direct methods using in WinGX package.<sup>32</sup> The treatment of hydrogen atoms was made geometrically. Supplementary material for structure has been deposited to the Cambridge Crystallographic Data Center as CCDC no: 1949380, 1949381 (deposit@ccdc.cam.ac.uk or http:// www.ccdc.cam.ac.uk).

#### 3. Results

#### 3. 1. X-Ray Studies

The Ortep drawing obtained from X-ray diffraction studies of complexes 1 and 2 were depicted in Figures 2 and 3. The crystal data and data collection conditions of

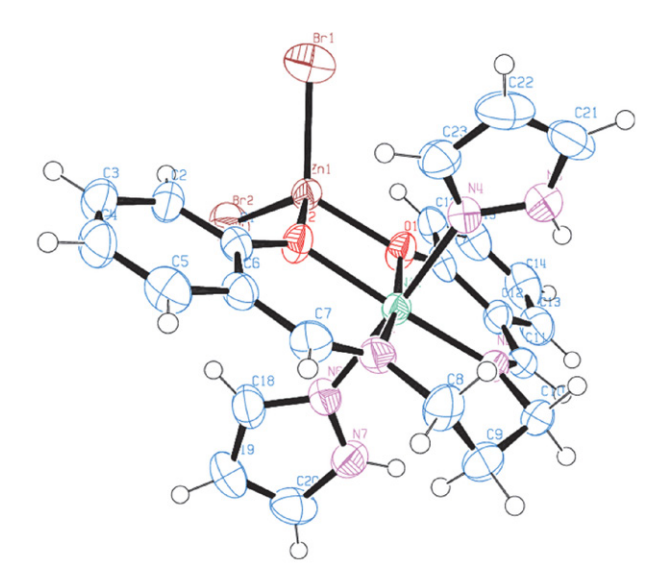


Figure 2. The Ortep drawing of 1.

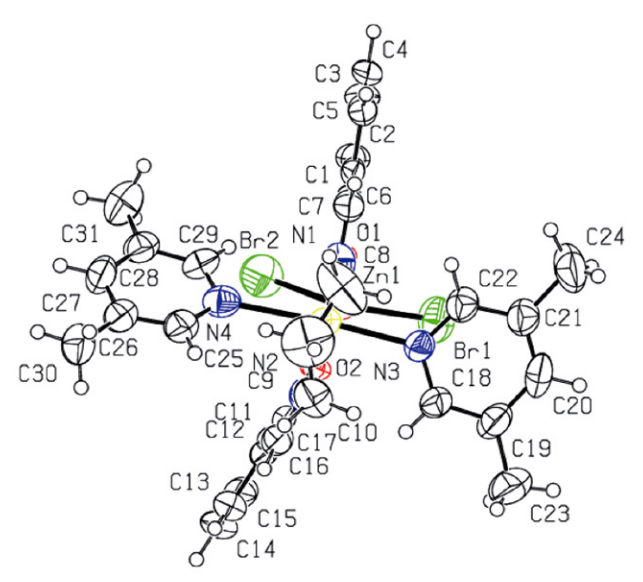


Figure 3. The Ortep drawing of 2.

these complexes were tabulated in Table 1, the bond lengths and the bond angles are shown in Table 2.

As seen in Figures 2 and 3, Ni(II) ion in both complexes is in an octahedral coordination sphere between the  $\rm O_2N_2$  donors of the Schiff base, pyrazole and the two nitrogens of lutidine. On the other hand, Zn(II) ions are located in a distorted tetrahedral coordination sphere between two phenolic oxygen and two bromine atoms. However, based on the angle values given in Table 2, it can be concluded that the distortion value of the coordination sphere is highly extensive. The bond lengths in the equatorial plane of the octahedral coordination sphere of 1, Ni(II) and donor atoms, are around 2 Å while the axial bond lengths change between 2.138 and 2.178 Å. The corresponding values are 2.154–2.338 Å for 2. The equatorial bond lengths of Ni(II) donor atom are approximately 2 Å while axial bond lengths

Table 1. Crystal data and data collection conditions.

	1	2	
Molecular Formula C	<sub>23</sub> H <sub>24</sub> Br <sub>2</sub> N <sub>6</sub> NiO <sub>2</sub> Zn	C <sub>31</sub> H <sub>34</sub> Br <sub>2</sub> N <sub>4</sub> NiO <sub>2</sub> Zr	
Molar mass/ g mol <sup>-1</sup>	700.38	778.52	
T/K	293(2)	293(2)	
Crystal System	Monoclinic	Monoclinic	
Space Group	$P2_1/n$	$P2_1/c$	
a /Å	9.0086(3)	9.1210(5)	
b/Å	15.7423(6)	18.9500(10)	
c /Å	18.2777(7)	18.9770(10)	
Alpha	90	90	
Beta	98.856(4)	101.916(6)	
Gamma	90	90	
$V/Å^3$	2561.17(16)	3209.4(3)	
Z	4	4	
Calc. Density/ g cm <sup>-3</sup>	1.816	1.611	
$\mu / mm^{-1}$	4.825	3.858	
F (000)	1392	1568	
Reflections Collected	11155	24685	
Reflections Unique	5229	7144	
R1, wR2 (2σ)	0.0591, 0.1678	0.0773, 0.1992	
R1, wR2 (all)	0.0835, 0.1868	0.1699, 0.2489	
Data / Parameters	5229/ 320	7144/370	
GOOF of F <sup>2</sup>	1.058	1.022	
Largest Difference Peak Hole /e Å <sup>-3</sup>	1.031, -1.866	1.072, -1.514	
CCDC No	1949380	1949381	

differ from each other. The lengths of the bond between pyrazole and lutidine nitrogen atoms indicate that the coligands are located axially in the octahedral coordination sphere. In fact, the largest angle among these three atoms is formed between these two atoms.

The angle of N4NiN6 in **1** was measured as 176.4° and the angle of N3NiN4 in **2** was measured as 175.4°. In addition, in the coordination of Zn(II) the bond angles for **1** were found to be between 121.44°–82.52° and 79.07°–117.95° for **2**, respectively, showing a high tetrahedron distortion for these compounds.

Pyrazole coligand participates in the coordination through a double bond nitrogen atom. The N-H nitrogen of the pyrazole ring does not participate in the coordination. Since the electron pair present on this atom is donated to the  $\pi$  system of the ring, there is no electron pair left to donate to Ni(II) ion.

#### 3. 2. Thermal Analysis

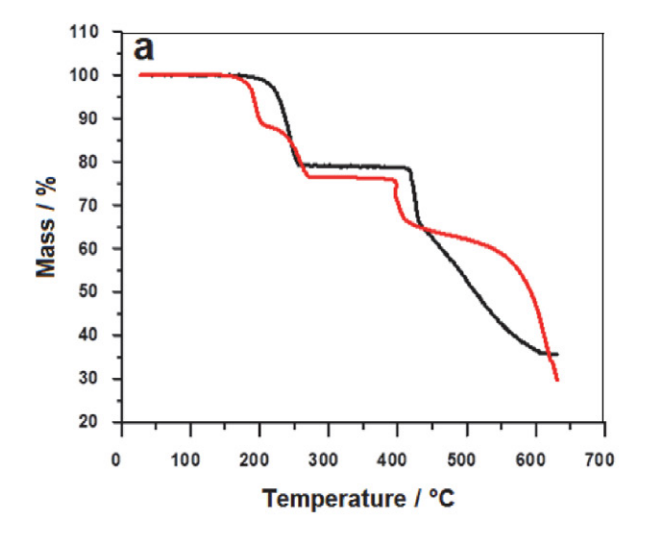
The TG and DTA curves of **1** and **2** are given in Figure 4. The thermoanalytical data of these complexes are tabulated in Table 3.

As can be seen from Figure 4 and Table 3, pyrazole coligands are separated from the structure in a single step. On the other hand, the removal of lutidine from the structure is a two-step process. In this process which is described as the first thermal reaction in Table 3, the coli-

**Table 2.** The selected bond lengths and angles around the coordination sphere of the complexes.

Bond Lengths / Å	Bond Angles / °
	1
N1-Ni1 2.027(5)	N7-N6-Ni1 125.8(5)
N2-Ni1 2.019(5)	Zn1-O1-Ni1 98.9(19)
N3-N4 1.336(8)	Zn1-O2-Ni1 99.0(19)
N4-Ni1 2.138(6)	N2-Ni1-N1 99.2(2)
N6-N7 1.324(8)	N2-Ni1-O2 170.0(2)
N4-Ni1 2.138(6)	N1-Ni1-O2 90.8(2)
N6-Ni1 2.178(6)	N2-Ni1-O1 90.6(2)
O1-Zn1 1.971(5)	N1-Ni1-O1 169.7(2)
O1-Ni1 2.042(5)	O2-Ni1-O1 79.5(18)
O2-Zn1 1.978(4)	N2-Ni1-N4 91.1(2)
O2-Ni1 2.031(4)	N1-Ni1-N4 87.4(2)
Ni1-Zn1 3.049(10)	O2-Ni1-N4 90.6(2)
Zn1-Br1 2.325(12)	O1-Ni1-N4 89.3(2)
Zn1-Br2 2.328(11)	N2-Ni1-N6 92.1(2)
	N1-Ni1-N6 90.6(2)
	O2-Ni1-N6 86.4(2)
	O1-Ni1-N6 92.1(2)
	N4-Ni1-N6 176.4(2)
	O1-Zn1-O2 82.5(18)
	O1–Zn1–Br1 119.6(15)
	O2-Zn1-Br1 109.2(15)
	O1–Zn1–Br2 113.1(15)
	O2–Zn1–Br2 121.4(15)
	Br1-Zn1-Br2 109.4(4)
	2
N1-Ni1 2.024(7)	N2-Ni1-O1 170.6(3)
N2-Ni1 2.004(8)	N2-Ni1-N1 98.9(3)
N3-Ni1 2.154(7)	O1-Ni1-N1 90.1(3)
N4-Ni1 2.338(8)	N2-Ni1-O2 92.0(3)
O1-Zn1 2.017(5)	O1-Ni1-O2 79.1(2)
O1-Ni1 2.020(5)	N1-Ni1-O2 169.1(3)
O2-Zn1 1.967(5)	N2-Ni1-N3 92.8(3)
O2-Ni1 2.030(5)	O1-Ni1-N3 89.6(2)
Ni1-Zn1 3.072(14)	N1-Ni1-N3 92.7(3)
Zn1-Br2 2.326(16)	O2-Ni1-N3 87.1(2)
Zn1-Br1 2.332(15)	N2-Ni1-N4 86.0(3)
	O1-Ni1-N4 90.9(3)
	N1-Ni1-N4 91.8(3)
	O2-Ni1-N4 88.4(2)
	N3-Ni1-N4 175.4(3)
	N2-Ni1-Zn1 130.9(2)
	O1-Ni1-Zn1 40.4(14)
	N1-Ni1-Zn1 130.2(2)
	O2-Ni1-Zn1 39.0(15)
	N3-Ni1-Zn1 83.5(19)
	N4-Ni1-Zn1 93.9(2)
	O2-Zn1-O1 80.6(2)
	O2-Zn1-Br2 112.2(16)
	O1-Zn1-Br2 110.7(16)

gands are removed from the structure leaving a NiL mononuclear complex and ZnBr<sub>2</sub> behind. The thermogravimetric curve of 1 depicted in Figure 4 displays a sin-



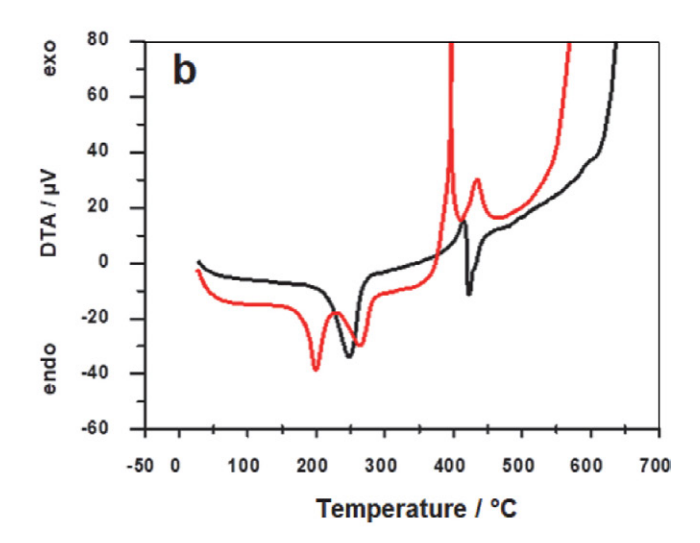


Figure 4. a. TG curves, b. DTA curves of 1 and 2 (black: 1, [NiL·ZnBr<sub>2</sub>·(pyrazole)<sub>2</sub>], red: 2, [NiL·ZnBr<sub>2</sub>·(3,5-lutidine)<sub>2</sub>].

Table 3. Thermoanalytical data of the complexes prepared.

Complex		1st Thermal Reaction Removal of coligands		2nd Thermal Reaction Decomposition of NiL residue		
	Temperature range / °C	Calcd mass loss / %	Final mass loss/ %	Temperature range / °C	Final mass loss/ %	
1	197–232	1st pyrazole loss: 9.71 Total loss: 19.42	Total loss: $20.10 \pm 0.58$	380-420	11.42 ± 1.27	
2	157-202-264	1st lutidine loss: 13.76 Total loss: 27.52	1st mass loss: 13.49 ± 0.35 2nd mass loss: 12.98 ± 0.77 Total loss: 26.47 ± 0.52	380-402	10.11 ± 2.17	

gle step endothermic mass loss between 197–232 °C corresponding to two pyrazole molecules (Table 3). The theoretically calculated mass of two pyrazole molecules in 1 was 19.42% while the experimentally determined value was 20.10%. Subsequently, a mass loss of about 10% was observed at around 380 °C which is the dissociation temperature of NiL mononuclear complex.<sup>23</sup>

The situation in **2** is entirely different. Two lutidine coligands in a complex molecule detach from the structure in two identical stages with two equal mass losses. The first mass loss of approximately 13.49% occurs in a temperature range of 157–202 °C. Subsequently, a second mass loss of 12.98% was observed between 202–264 °C. Since the mass of lutidine is 13.76% of the mass of the complex, lutidines

leave the structure one by one by two consecutive endothermic reactions. The residual NiL and ZnBr<sub>2</sub> mixture gives a mass loss of 10% at 380 °C corresponding to the dissociation of NiL complex.

#### 3. 3. Computational Results

The relative energy levels of HOMO and LUMO, dipole moments and formation energies obtained by using the sets in the Gaussian 09 program are given in Table 4. The orbital occupation values of the donor atoms are tabulated in Table S1 and the types of orbitals are given in Table S2. Figure 5 shows ESP maps and HOMO-LUMO images of the complexes.

Table 4. The relative energy levels of HOMO and LUMO, dipole moments and formation energies of the complexes prepared in the study, calculated with Gaussian 09.

Complex	E <sub>HOMO</sub> / eV	E <sub>LUMO</sub> / eV	ΔE / eV	μ/D	IP / eV	E <sub>A</sub> /eV	ΔH° <sub>f</sub> /kJ mol <sup>-1</sup>
1	-6.167	-2.569	3.598	12.947	6.167	2.569	2173.76
2	-6.070	-2.497	3.573	12.501	6.070	2.497	2113.91

Optimization – b3lyp/6-31G(d), NImag: 0, IP: ionization potential, EA: electron affinity

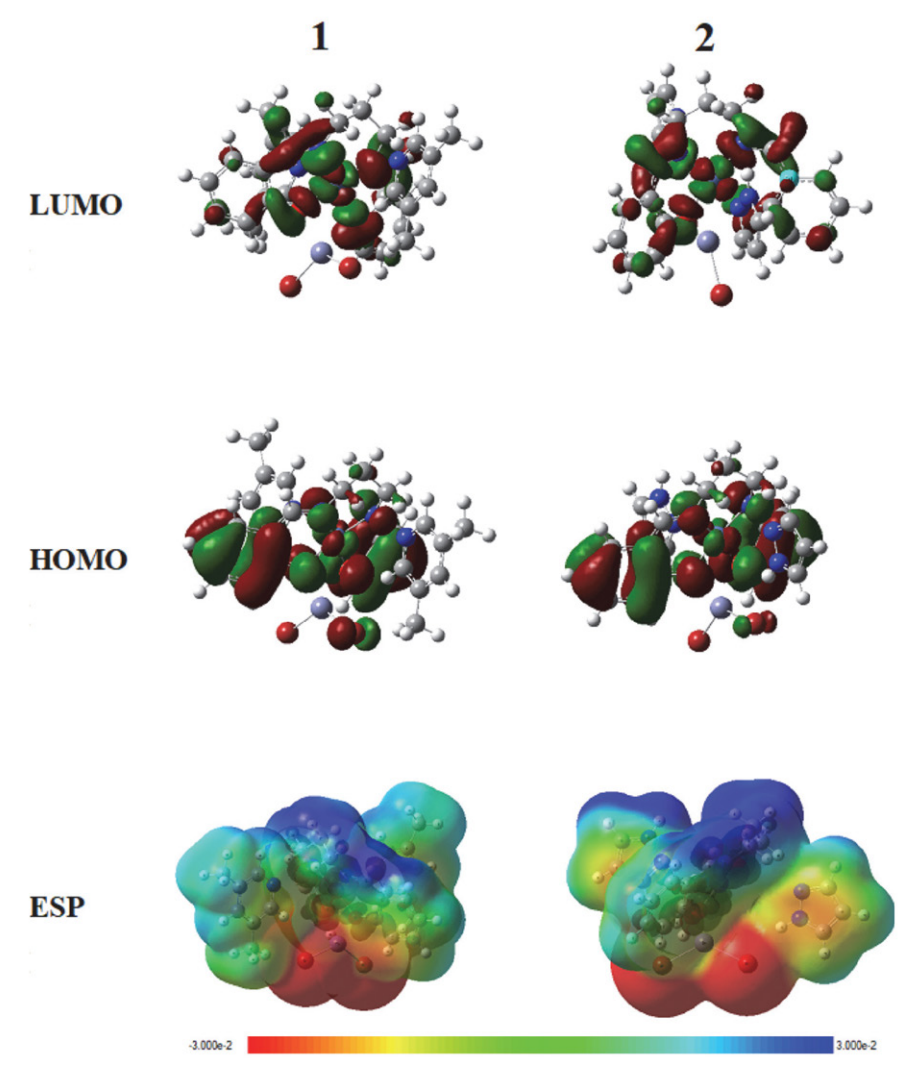


Figure 5. HOMO-LUMO images and ESP maps of the complexes.

The dipole moments, formation enthalpies and relative energy levels of HOMO and LUMO of the complexes came out to be highly similar. This is a highly expected outcome since the two complexes are very similar to each other. In both complex Ni(II)ion is in  $O_2N_4$  octahedral coordination sphere while Zn(II) is located in a neighboring tetrahedral  $O_2Br_2$  coordination sphere. Pyrazole and lutidine donate electrons to Ni(II) ion while Zn(II) ion attracts the electrons towards bromine atoms via phenolic oxygens. That is why chelate rings assume partially positive and bromine atoms partially negative charges as clearly seen in ESP maps given in Figure 5.

Since the diameter of the molecule is large, it is quite normal for the dipole moment to be high. Among the data obtained from NBO studies, the electron occupation values indicate that Ni(II) ion is in octahedral coordination. When focusing on Ni(II) ions, it can easily be seen that three d orbitals are occupied and the remaining two contain empty sites. This is expected for the octahedral crystal

field splitting theory. On the other hand, Zn(II) possesses 10 d electrons, all d orbitals were found to be filled. There are two nitrogen atoms in the pyrazole ring. One of the nitrogen atoms has a hydrogen atom and an electron pair, the other one attached to the ring with a double bond. However, both nitrogens donate electrons to the  $\pi$  system of the aromatic ring and there are unfilled p orbitals in nitrogen atoms in the ring. This distribution is more homogeneous in iminic nitrogens.

#### 4. Discussion

The difference between the two complexes is not clear from IR data. The most important result from IR data is the difference between the C=N vibrations of the ligand and the complexes. While C=N vibration was observed at 1608 cm<sup>-1</sup> in ligand, it was observed at 1598 and 1595 cm<sup>-1</sup> in complexes. This data proves that iminic nitrogen is co-

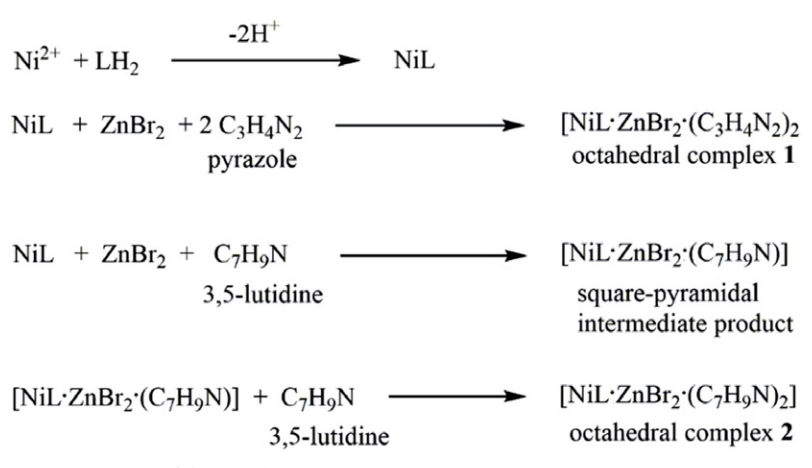
ordinated to the structure. It is already known that when the imine nitrogen is coordinated to a metal, the stretch vibration shifts to a low energy by 10–30 cm<sup>-1</sup>. Apart from this, O–H stretches observed around 2600 cm<sup>-1</sup> due to the strong hydrogen bonds are not observed in the complex spectra. In complexes, vibrations between nitrogen and metal ion in coligands cannot be determined from the spectra because IR spectra were recorded with ATR equipment and it is not possible to observe vibrations less than 600 cm<sup>-1</sup> with ATR. However, in the theoretical calculations, the Ni–N(pyrazole) stretches can be observed at 334 cm<sup>-1</sup> for 1, at 450 cm<sup>-1</sup> for 2; the Ni–N(imine) stretches can be observed at 423 cm<sup>-1</sup> for 1, at 472 cm<sup>-1</sup> for 2; the Ni–O(phenol) stretches can be observed at 623 cm<sup>-1</sup> for 1, at 602 cm<sup>-1</sup> for 2 (Figure S1).

The most important difference between the complexes is the variation of coordinative bond lengths observed in X-ray diffraction patterns. In 1, the pyrazole molecule is attached to Ni(II) with electron pair of the non-hydrogen bonded nitrogen atom of the pyrazole ring. The distance between two pyrazoles with Ni(II) ion is very close to each other, as seen in Table 2, these distances are 2.138 and 2.178 Å. However, the situation is different in 2. The two lutidines have different distances to Ni(II) ion. These distances are found to be 2.154 Å and 2.338 Å. This is also seen in the TG and DTA curves. As can be seen in Figure 4, both pyrazole coligands in 1 leave the structure in a single-stage process. The same situation is not valid for 2, the removal of lutidine from the complex structure takes place in two distinctive stages. This shows that the coordinative effects of pyrazole and lutidine are different, lutidine is a stronger ligand than pyrazole. This is an expected result because the pyrazole ring is a more acidic and electron-withdrawing group,<sup>34</sup> lutidine is a better electron-donating ligand. If the phenolic oxygens of NiL unit coordinate a Lewis acid, the electrons of phenolic oxygen are attracted by Lewis acid resulting in the decrease of the electron density around the Ni(II) ion provided by the phenolic oxygens of the ligand to Ni(II) ion. Under this

condition, Ni(II) ion compensates for the decreasing electron density by the coordination of solvent molecules or coligands present in the medium. If the electrons provided by a single coligand are sufficient, a square pyramidal coordination sphere is formed. If the electrons provided are not sufficient, then an octahedral coordination sphere occurs by the coordination of two coligands. In fact, in similar studies carried out by picoline, there were square-pyramidal or octahedral coordination spheres formed depending upon the picoline concentration.<sup>28</sup> If the coligand concentration in the medium is sufficiently high then an octahedral coordination sphere is formed by the addition of a new coligand to the square pyramidal structure of Ni(II) ion (Scheme 1).

This situation is clearly illustrated in Figure 4. While the pyrazole molecules are thermally discarded from the structure with a single-stage process, this takes in two distinctive processes in the case of lutidine. Therefore, the distance of the lutidine molecules to Ni(II) ion is different. DTA curves verify the fact that lutidine molecules are removed from the structure by two distinctive endothermic reactions. The total mass loss observed in these endothermic reactions is approximately equal to the mass of two lutidine molecules. Similarly, in the case of using pyrazole as a coligand, the mass loss in a single endothermic reaction is equal to the mass of two pyrazole molecules.

The visual observation of the chelate rings that occurred in both complexes showed that they have semichair conformation. Both complexes give a six-membered chelate ring with two nitrogen molecules of the Schiff base, a trimethylene bridge connecting to these two nitrogen atoms, and a central Ni(II) ion. The interplanar angles were calculated by the use of Parst program.<sup>35</sup> For 1, the angle between the atomic planes of C8–C9–C10 and C8–N1–N2–C10 was 62.85°, the angle between C8–N1–N2–C10 and N1–Ni1–N2 was 7.35°. The ideal value of these angles in chair conformation is 62°. Under these conditions, one side of the chelate ring is in a stressed position and it appears to be a semi-chair structure.



Scheme 1. Schematic preparation reactions of the complexes.

On the other hand, for **2** these angles are 50.74 and 10.77°. In both complexes, the aromatic rings of the coligands are not in the same plane. The angle between the two pyrazole planes in **1** is 20.74° and the angle between two lutidine planes in **2** is 57.39° (Figure 1). These values are similar to the data in the literature, the angles between the N1-Ni-N2 plane and C8-N1-N2-C9 plane have been reported between 5.0 and 8.9°.<sup>23,24,36</sup>

The theoretical study results, unfortunately, do not clearly show the difference between the complexes. Almost all the values of the two complexes are quite close to each other. The energy differences of HOMO-LUMO orbitals and dipole moments are approximately the same in these two complexes. The electron occupation values in the d orbitals of Ni(II) ion obtained from NBO analysis are close. In these two complexes, the occupation values of the  $d_{xy}$  $d_z^2$ ,  $d_x^2 - v^2$  orbitals are the same, only there is a slight difference in the  $d_{vz}$  and  $d_{zx}$  orbitals. As can be seen from Table 5, the occupancy value of the  $d_{vz}$  orbital for 1 is 1.14 electrons, the  $d_{zx}$  orbital is 1.60 electrons, the same orbitals have occupancy levels of 1.02 and 1.71 electrons in 2. This result shows that the energy of the d<sub>vz</sub> orbital in 2 is higher and according to the crystal field theory, the lutidine coligand offers more electrons to Ni(II) central ion. However, the difference is not significant and the second-order perturbation results in the NBO analysis reveal that there is no difference between the numerical values obtained from the two complexes and it is not possible to determine the electron donation effects of the coligands from the theoretical calculations, but at this point, thermal analysis brings an advantage. It is possible to interpret the difference between the strengths of the two coligands using thermogravimetric results. The stronger electron-donating coligand lutidine can form an intermediate stable compound of [NiL·ZnBr<sub>2</sub>·(3,5-lutidine)] in the dinuclear complex, although a pyrazole molecule cannot offer enough electrons, [NiL·ZnBr<sub>2</sub>·(pyrazole)] molecule does not form, instead [NiL·ZnBr<sub>2</sub>·(pyrazole)<sub>2</sub>] complex is formed with two pyrazole molecules. In this study, the complex was prepared at different 3,5-lutidine concentrations, but all the complex stoichiometries obtained were [NiL·Zn- $Br_2 \cdot (3.5 - lutidine)_2$  and  $[NiL \cdot ZnBr_2 \cdot (3.5 - lutidine)]$  could not be prepared. However, thermogravimetry shows that this complex can be prepared. This work also proves the importance of thermogravimetry in the study of complexes.

#### 5. Conclusion

Lewis acids can attract electrons from the oxygens of the coordination sphere of bis-*N*,*N*'-salicylidene-1,3-propanediamine-Ni(II) complex forming polynuclear  $\mu$ -complexes. This results in a decrease of the electron density upon Ni(II) ion. Therefore, Ni(II) ion coordinates the solvent molecules or the coligands present in the medium by

withdrawing electrons. If the coligand possesses a sufficiently high electron density, it forms a square pyramidal coordination sphere. If the electron density of the coligand is not sufficiently high, then Ni(II) ion attaches two coligands forming an octahedral coordination sphere.

#### Acknowledgments

This research did not receive any specific grant from funding agencies. The authors (Y. Gürsoy Tuncer and K. Gürpınar) thank to The Scientific and Technological Research Council of Turkey (TUBITAK) for financial support (Project number: 118F128). The authors declare that there is no conflict of interest.

#### 6. References

- C. Fukuhara, K. Tsuneyoshi, N. Matsumoto, S. Kida, M. Mikuriya, M. Mori, *Dalton Trans.* 1990, 11, 3473–3479; DOI:10.1039/DT9900003473
- A. Gerli, K. S. Hagen, L. G. Marzilli, *Inorg. Chem.* 1991, 30, 4673–4676; DOI:10.1021/ic00024a043
- S. Mirdya, M.G.B. Drew, A.K. Chandra, A. Banerjee, A. Frontera, S. Chattopadhyay, *Polyhedron* 2020, *179*, 114374;
  DOI:10.1016/j.poly.2020.114374
- S. Uhlenbrock, R. Wegner, B. Krebs, *Dalton Trans.* 1996, 18, 3731–3736; DOI:10.1039/dt9960003731
- F. Ercan, O. Atakol, C. Arıcı, I. Svoboda, H. Fuess, *Acta Crystallogr. C* 2002, 58, 193–196; DOI:10.1107/S0108270102001609
- 6. T. G. Dastidar, S. Chattopadhyay, *Polyhedron* **2022**, *211*, 115511; **DOI**:10.1016/j.poly.2021.115511
- Y. Li, L. Xu, M. Duan, B. Zhang, Y. Wang, Y. Guan, J. Wu, C. Ling, Z. You, *Polyhedron* 2019, 166, 146–152;
  DOI:10.1016/j.poly.2019.03.051
- 8. S. Ghosh, G. Aromi, P. Gamez, A. Ghosh, *Eur. J. Inorg. Chem.* **2015**, *18*, 3028–3037; **DOI**:10.1002/ejic.201500273
- S. Öz, Ü. Ergun, M. Yakut, I. Svoboda, A. Atakol, E. K. İnal, N. Yılmaz, O. Atakol, Russ. J. Coord. Chem. 2014, 40, 571–582;
  DOI:10.1134/S1070328414080089
- Y. N. Chen, Y. Y. Ge, W. Zhou, L. F. Ye, Z. G. Gu, G. Z. Ma,
  W. S. Li, H. Li, Y. P. Cai, *Inorg. Chem. Commun.* 2011, 14,
  1228–1232; DOI:10.1016/j.inoche.2011.04.028
- C. Arıcı, D. Ülkü, O. Atakol, *Anal. Sci.* 2002, 18, 959–960;
  DOI:10.2116/analsci.18.959
- A. Finelli, N. Herault, A. Crochet, K. M. Fromm, *Cryst. Growth Des.* 2018, *18*, 1215–1226;
  DOI:10.1021/acs.cgd.7b01769
- 13 S. Ghosh, A. Ghosh, *Inorg. Chim. Acta.* **2016**, 442, 64–69; **DOI**:10.1016/j.ica.2015.11.029
- 14. O. Atakol, L. Tatar, M. A. Akay, D. Ülkü, *Anal. Sci.* **1999**, *15*, 101–102; **DOI**:10.2116/analsci.15.101
- 15. P. Seth, A. Figuerola, J. Jover, E. Ruiz, A. Ghosh, *Polyhedron* **2016**, *117*, 57–63; **DOI:**10.1016/j.poly.2016.05.021
- A. Hazari, A. Das, P. Mahapatra, A. Ghosh, *Polyhedron* 2017, 134, 99–106; DOI:10.1016/j.poly.2017.06.007

- A. Hazari, K. J. Gomez-Garcia, M. G. B. Drew, A. Ghosh, *Polyhedron* 2017, *138*, 145–153; DOI:10.1016/j.poly.2017.09.012
- R. Kurtaran, L. T. Yıldırım, A. D. Azaz, H. Namli, O. Atakol, *J. Inorg. Biochem.* 2005, 99, 1937–1944;
  DOI:10.1016/j.jinorgbio.2005.05.016
- A. Hazari, L. K. Das, A. Bauza, A. Frontera, A. Ghosh, *Dalton Trans.* 2016, 45, 5730–5740; DOI:10.1039/C5DT04941E
- A. Hazari, S. Giri, C. Diaz, A. Ghosh, *Polyhedron* 2016, 118, 70–80; DOI:10.1016/j.poly.2016.07.035
- M. Aksu, S. Durmuş, M. Sarı, K. C. Emregül, I. Svoboda, H. Fuess, O. Atakol, *J. Therm. Anal. Calorim.* 2007, 90, 541–547;
  DOI:10.1007/s10973-006-7729-5
- M. Sönmez, H. Nazır, E. Emir, I. Svoboda, L. Aksu, O. Atakol, *J. Therm. Anal. Calorim.* 2018, *131*, 3077–3091;
  DOI:10.1007/s10973-017-6720-7
- A. Atakol, H. Nazır, I. Svoboda, M. L. Aksu, O. Atakol, J. Therm. Anal. Calorim. 2020, 139, 1863–1882;
  DOI:10.1007/s10973-019-08630-w
- M. G. B. Drew, R. N. Prasad, R. P. Sharma, Acta Crystallogr. C 1985, 41, 1755–58; DOI:10.1107/S0108270185009337
- Y. Elerman, M. Kabak, O. Atakol, Acta Crystallogr. C 1993, 49, 1905–1906; DOI:10.1107/S0108270193004615
- O. Atakol, C. Arıcı, F. Ercan, D. Ülkü, Acta Crystallogr. C
  1999, 55, 511–513; DOI:10.1107/S0108270198014334

- 27. S. Biswas, C. Diaz, A. Ghosh, *Polyhedron* **2013**, *51*, 96–101; **DOI**:10.1016/j.poly.2012.12.019
- O. Atakol, H. Nazır, C. Arıcı, S. Durmuş, I. Svoboda, H. Fuess, *Inorg. Chim. Acta* 2003, 342, 295–300;
   DOI:10.1016/S0020-1693(02)01163-5
- 29. M. J. Frisch, G. W. Trucks, H. B. Schlegel, G. E. Scuseria, M. A. Robb, J. R. Cheeseman, G. Scalmani, V. Barone, B. Mennucci, G. Petersson, H. Nakatsuji: Gaussian 09, Revision D. 01, Gaussian. Inc., Wallingford CT, 2009.
- CrysAlis C. CrysAlis RED, Version 1.171. Oxford Diffraction Ltd., Abdingdon, UK, 2002.
- 31. G. M. Sheldrick, *Acta Cryst. C* **2015**, *71*, 3–8; **DOI:**10.1107/S2053229614024218
- L. J. Farrugia, J. Appl. Crystallogr. 1999, 32, 837–838;
  DOI:10.1107/S0021889899006020
- N. Acar, O. Atakol, Ş. B. Sopacı, D. C. Duman, I. Svoboda, S. Öz, J. Therm. Anal. Calorim. 2017, 127, 1319–1327;
  DOI:10.1007/s10973-016-6004-7
- 34. J. A. Joule, K. Mills: Heterocyclic Chemistry, Wiley-VCH, Weinheim, Germany, **2010**, pp. 485–488.
- A. L. Spek, Acta Crystallogr. D 2009, 65, 148–155;
  DOI:10.1107/S090744490804362X
- F. Akhtar, M. G. B. Drew, Acta Crystallogr. B 1982, 38, 1149–1152; DOI:10.1107/S0567740882005184

#### Povzetek

Enojedrni kompleks NiL smo pripravili z uporabo bis-N,N-saliciliden-1,3-propandiamina in Ni(II) soli. NiL smo reagirali s  $ZnBr_2$ , pirazolom in 3,5-lutidinom kot soligandoma v dioksanu in izolirali diheterojedrna kompleksa:  $[NiL \cdot ZnBr_2 \cdot (pyrazole)_2]$  in  $[NiL \cdot ZnBr_2 \cdot (3,5-lutidine)_2]$ . Kompleksa smo okarakterizirali z elementno analizo, TG, IR in masno spektrometrijo. Proučili smo učinek heterocikličnih ligandov. Z uporabo programa Gaussian09 smo izračunali tvorbene entalpije, dipolne momente ter energije HOMO in LUMO orbital. Zasedenost atomskih orbital smo določili z NBO analizo. Vpliv pirazola in lutidina na tvorbo kompleksa smo ovrednotili z uporabo rentgenske difrakcije, TG in teoretičnih izračunov. Kompleks NiL z lutidinom tvori kvadratno piramidalno konformacijo, saj je lutidin veliko močnejši koligand kot pirazol.



Except when otherwise noted, articles in this journal are published under the terms and conditions of the Creative Commons Attribution 4.0 International License